Human Genetics (2019) 138:151–166
https://doi.org/10.1007/s00439-019-01969-y

ORIGINAL INVESTIGATION

LncRNA ZBTB40-IT1 modulated by osteoporosis GWAS risk SNPs suppresses osteogenesis

Bing Mei[1] · Ya Wang[1] · Weiyuan Ye[1] · Han Huang[1] · Qian Zhou[1] · Yuanyuan Chen[1] · Yajing Niu[1] · Manling Zhang[1] · Qingyang Huang[1]

Received: 12 October 2018 / Accepted: 2 January 2019 / Published online: 19 January 2019

Abstract

Previous genome-wide linkage and association studies have identified an osteoporosis-associated locus at 1p36 that harbors SNPs rs34920465 and rs6426749. The 1p36 locus also comprises the *WNT4* gene with known role in bone metabolism and functionally unknown *ZBTB40*/lncRNA *ZBTB40-IT1* genes. How these might interact to contribute to osteoporosis susceptibility is not known. In this study, we show that lncRNA ZBTB40-IT1 is able to suppress osteogenesis and promote osteoclastogenesis by regulating the expression of *WNT4, RUNX2, OSX, ALP, COL1A1, OPG* and *RANKL* in U-2OS and hFOB1.19 cell lines, whereas *ZBTB40* plays an opposite role in bone metabolism. Treatment with parathyroid hormone significantly downregulates the expression of *ZBTB40-IT1* in U-2OS cell lines. *ZBTB40* can suppress *ZBTB40-IT1* expression but has no response to parathyroid hormone treatment. Dual-luciferase assay and biotin pull-down assay demonstrate that osteoporosis GWAS lead SNPs rs34920465-G and rs6426749-C alleles can respectively bind transcription factors JUN::FOS and CREB1, and upregulate *ZBTB40* and *ZBTB40-IT1* expression. Our study discovers the critical role of *ZBTB40* and lncRNA ZBTB40-IT1 in bone metabolism, and provides a mechanistic basis for osteoporosis GWAS lead SNPs rs34920465 and rs6426749.

Introduction

Osteoporosis is a common complex disease defined by bone mineral density (BMD) that is highly heritable with the heritability estimates of 0.5–0.85 (Ralston et al. 2010). The discovery of genetic variation loci and elucidation of their biological functions for BMD variations are important in understanding the etiology of osteoporosis and in developing new approaches for osteoporosis screening, prevention and treatment. Multiple genome-wide linkage scans have shown that 1p36 is one of the strongest linkage genomic regions to BMD across populations (Devoto et al. 1998, 2001; Streeten et al. 2006). 1p36.12 was identified by an initial large-scale BMD genome-wide association study (GWAS) (Styrkarsdottir et al. 2008) and further replicated by multiple GWAS meta-analyses (Estrada et al. 2012; Kemp et al. 2014; Rivadeneira et al. 2009; Styrkarsdottir et al. 2009; Zhang et al. 2014; Zheng et al. 2015). The reported SNPs included intron SNPs rs2708632, rs75077113, rs6701290, rs3765350, rs2235529, rs4589135 and intergenic SNPs rs3920498, rs12755933, rs34920465, rs6696981 and rs6426749. A three-stage GWAS meta-analysis in 27,061 study subjects confirmed that SNP rs34920465 was strongly associated with BMDs at the lumbar spine, hip and femoral neck ($P = 2.67 \times 10^{-13}$) (Zhang et al. 2014). SNP rs6426749 not only showed significant associations with femur neck, lumbar spine and hip BMD in the Europeans and East-Asians ($P = 7.6 \times 10^{-10}$) (Kim et al. 2016; Park et al. 2014; Rivadeneira et al. 2009; Styrkarsdottir et al. 2010), but also presented significant association for BMD global Wald test (Warrington et al. 2015). Most of these GWAS-SNPs have not been functionally characterized in vitro or in vivo yet. A recent study showed that rs6426749 can bind transcription factor TFAP2A and act as a distal allele-specific enhancer modulating the expression of *LINC00339* via long-range chromatin loop formation (Chen et al. 2018).

WNT4, ZBTB40 and *ZBTB40-IT1* genes are located in the 1p36 locus. WNT4 could promote osteoblast differentiation of mesenchymal stem cells (MSCs) (Chang et al. 2007) and

Electronic supplementary material The online version of this article (https://doi.org/10.1007/s00439-019-01969-y) contains supplementary material, which is available to authorized users.

✉ Qingyang Huang
huangqy@mail.ccnu.edu.cn

[1] Hubei Key Laboratory of Genetic Regulation and Integrative Biology, School of Life Sciences, Central China Normal University, Wuhan 430079, China

attenuate bone loss in osteoporosis and skeletal aging mouse models by inhibiting nuclear factor-κB via noncanonical WNT signaling (Yu et al. 2014). LncRNA ZBTB40-IT1 is generated by alternative splicing of an intron of *ZBTB40*. The functional roles of *ZBTB40* and *ZBTB40-IT1* in bone metabolism are unknown. Notablely, a recent study found that *CDC42* and *LINC00339* are the target genes of the rs6426749 in the 1p36 locus (Chen et al. 2018). CDC42 is a key regulator of cytoskeletal components and a crucial component of the pivotal MAPK pathway of bone metabolism (Greenblatt et al. 2013), and has the important roles in bone modeling and remodeling (Ito et al. 2010). Deletion of *Cdc42* in mice decreased bone formation (Wuerfel et al. 2012), and showed severe skeletal abnormalities (Aizawa et al. 2012), *LINC00339* with unknown function in bone metabolism could negatively regulate the expression of *CDC42* (Powell et al. 2016; Chen et al. 2018).

LncRNAs are noncoding transcripts with more than 200 nucleotides in length. Growing evidences show that lncRNAs are important regulators of osteoporosis pathophysiology processes. For example, LncRNA MEG3 was up-regulated in bone marrow MSCs from postmenopausal osteoporosis, and could repress osteogenic differentiation by targeting miR-133a-3p (Wang et al. 2017a, b). H19 functioned as a competing endogenous RNA, which promoted osteoblast differentiation via the activation of Wnt signaling (Huang et al. 2015; Liang et al. 2016). Upregulation of HIF1α-AS1 can promote osteoblastic differentiation of bone marrow MSCs by blocking the expression of *HOXD10* (Xu et al. 2015). Whether lncRNA ZBTB40-IT1 at 1p36 plays a vital role in osteoporosis is unclear.

In this study, we explored the functional roles of *ZBTB40* and *ZBTB40-IT1* in bone metabolism, and found that lncRNA ZBTB40-IT1 suppress osteogenesis and promote osteoclastogenesis by regulating the expression of *WNT4, RUNX2, OSX, ALP, COL1A1, OPG* and *RANKL*, whereas *ZBTB40* has an opposite effect. We also demonstrated that osteoporosis GWAS lead SNPs rs34920465 and rs6426749 at 1p36 can modulate *ZBTB40-IT1* and *ZBTB40* expression via differential binding of bone metabolism related transcriptional factors JUN::FOS and CREB1, respectively.

Materials and methods

Cell lines, cell culture and PTH treatment

Two human osteosarcoma cell lines Saos-2 and U-2OS and a human embryonic kidney cell line HEK293T were obtained from the Cell Bank of Wuhan University (Wuhan, China). The human osteoblast cell line hFOB1.19 was purchased from the Cell Bank of Chinese Academy of Sciences (Shanghai, China). Saos-2 cells were cultured in MEM medium (HyClone, Waltham, MA, USA), U-2OS cells were grown in McCOY'S 5A medium (HyClone, Waltham, MA, USA) and 293T cells were maintained in DMEM medium (HyClone, Waltham, MA, USA). Media were supplemented with 2 mM L-glutamine and 4 mM GlutaMAX™ (Gibco, Grand Island, NY, USA), 10% fetal calf serum (Si Jiqing Co., Hangzhou, China), 100 units/ml penicillin and 100 µg/ml streptomycin (Gibco, Grand Island, NY USA). These three cell lines were cultured in an atmosphere of 5% CO_2 at 37 °C with 100% relative humidity. hFOB1.19 cells were cultured in DME/F-12 (1:1) medium (HyClone, Waltham, MA, USA) containing 10% fetal bovine serum (Gibco, Grand Island, NY USA), 0.3 mg/ml G418 (Sangon Biotech, Shanghai, China), 100 units/ml penicillin and 100 µg/ml streptomycin (Gibco, Grand Island, NY, USA), and maintained at the permissive temperature of 33.5 °C with 5% CO_2 for a rapid cell division.

U-2OS cells were seeded onto a six-well plate. After 90% confluence, the cells were treated with PTH (25 nM or 50 nM) for 8 h, 12 h, 16 h, 20 h, and vehicle as a control. Then cells were harvested for RNA extraction.

Reagents and antibodies

Human parathyroid hormone (1–34): Phoenixpeptide (Burlingame, USA, #055-08), Pierce BCA Protein Assay Kit (CWBiotech, Beijing, China), TRIzol Reagent (Life Technologies), Ultrapure RNA Kit (CWBiotech, Beijing, China), RIPA lysis buffer (CWBiotech, Beijing, China), Protease inhibitor cocktail (Sigma-Aldrich, Germany, #P8340), Neofect™ DNA transfection reagent (Neofect Biotech, Beijing, China), Lipofectamine® 3000 reagent (Invitrogen), Dual-Glo Assay system (Promega, USA, E1910). The primary antibodies were purchased from the following sources: anti-WNT4 (sc-13962, Santa Cruz), anti-RUNX2 (sc-12488, Santa Cruz), anti-OSX (sc-22538, Santa Cruz), anti-OPG (sc-11383, Santa Cruz), anti-RANKL (sc-9073, Santa Cruz), anti-CREB1 (sc-58, Santa Cruz; #9197, Cell Signaling Technology), anti-JUN (sc-1694, Santa Cruz; #9165, Cell Signaling Technology) and α-TUBULIN (sc-5546, Santa Cruz). Near-Infrared Fluorescent secondary antibodies (LI-COR Biotechnology, Lincoln, NE, USA).

Genotyping of GWAS SNPs in four cell lines

PCR-seq method was used to obtain genotype of rs34920465 and rs6426749 in U-2OS cells, Saos-2 cells, HEK293T cells and hFOB1.19 cells. A 500-bp sequence centered on rs34920465 or rs6426749 was PCR amplified from the four cells genomic DNA respectively using primers listed in Table S1. The SNPs rs34920465 and rs6426749 were subsequently genotyped by sequencing the amplified DNAs.

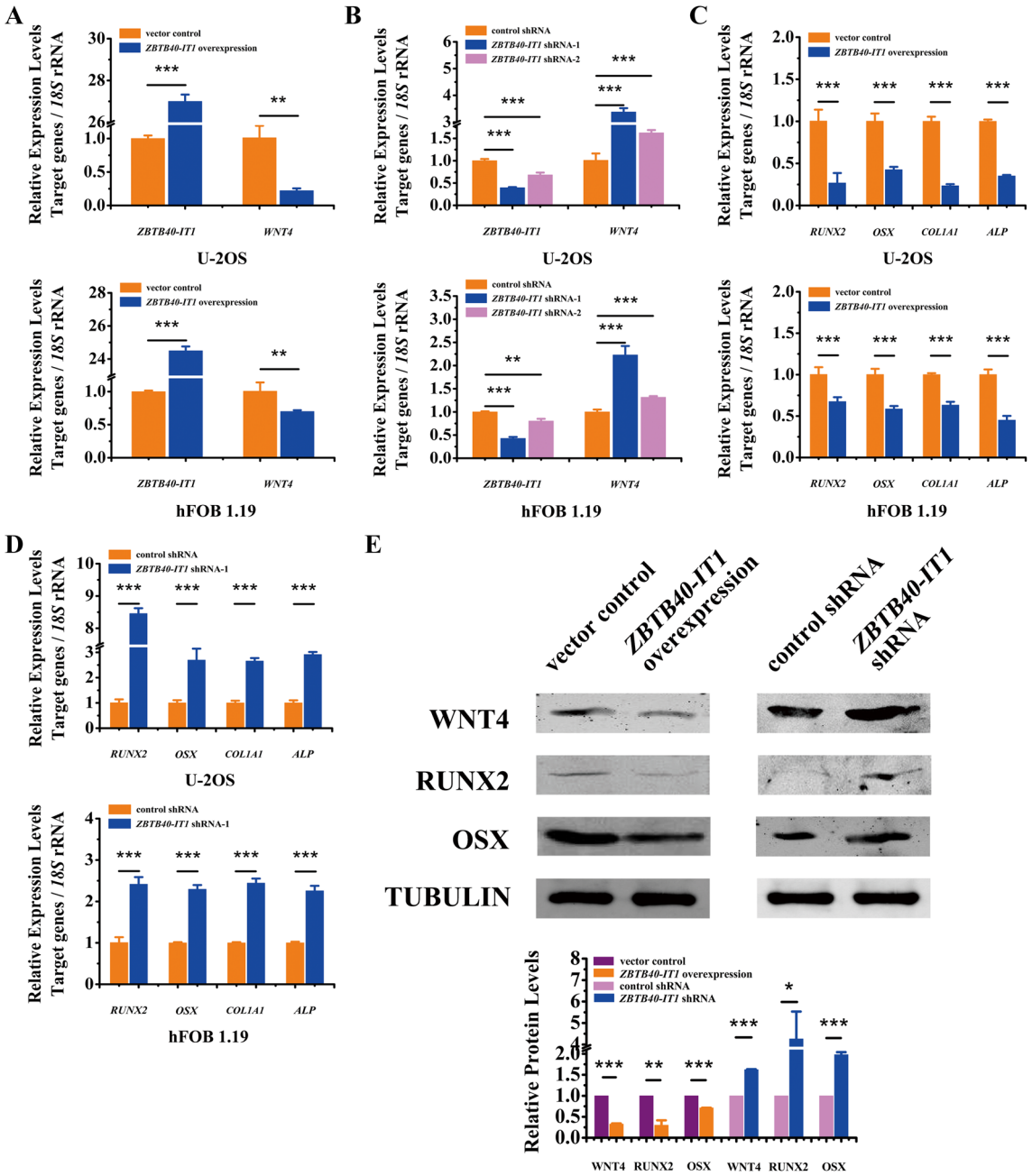

Fig. 1 Effect of LncRNA ZBTB40-IT1 on expression of *WNT4* and osteogenesis related genes. **a** Overexpression of *ZBTB40-IT1* substantially diminished *WNT4* expression in U-2OS and hFOB1.19 cells. **b** The shRNA-mediated reduction of *ZBTB40-IT1* (shRNA-1 and shRNA-2: two different shRNAs, blue and carmine) increased *WNT4* expression in U-2OS and hFOB1.19 cells. Relative expression of osteogenesis related gene *RUNX2, OSX, COL1A1* and *ALP* after overexpression (**c**) or shRNA-mediated knockdown (**d**) of *ZBTB40-IT1* as measured by real-time qRT-PCR. **e** Immunoblot analysis of WNT4, RUNX2 and OSX with overexpression or shRNA-mediated knockdown of *ZBTB40-IT1* in U-2OS cells and gray-scale analyses of the protein bands. Error bars show the standard deviation for five technical replicates of a representative experiment. *P* values were calculated by a two-tailed Student's *t* test. $^{**}P < 0.01$, $^{***}P < 0.001$

Plasmid constructs and site-directed mutagenesis

To avoid false negative results,we choose a relatively long fragment surrounding the corresponding SNP to evaluate the potential bidirectional regulatory function. DNA fragments containing rs6426749 (3.4-kb) and rs34920465 (3.5-kb) were separately amplified by PCR using 293T cell genomic DNA as templates. The resulting PCR products were then digested and cloned into luciferase reporter vector pGL3 promoter (Promega, Madison, USA). Fragments

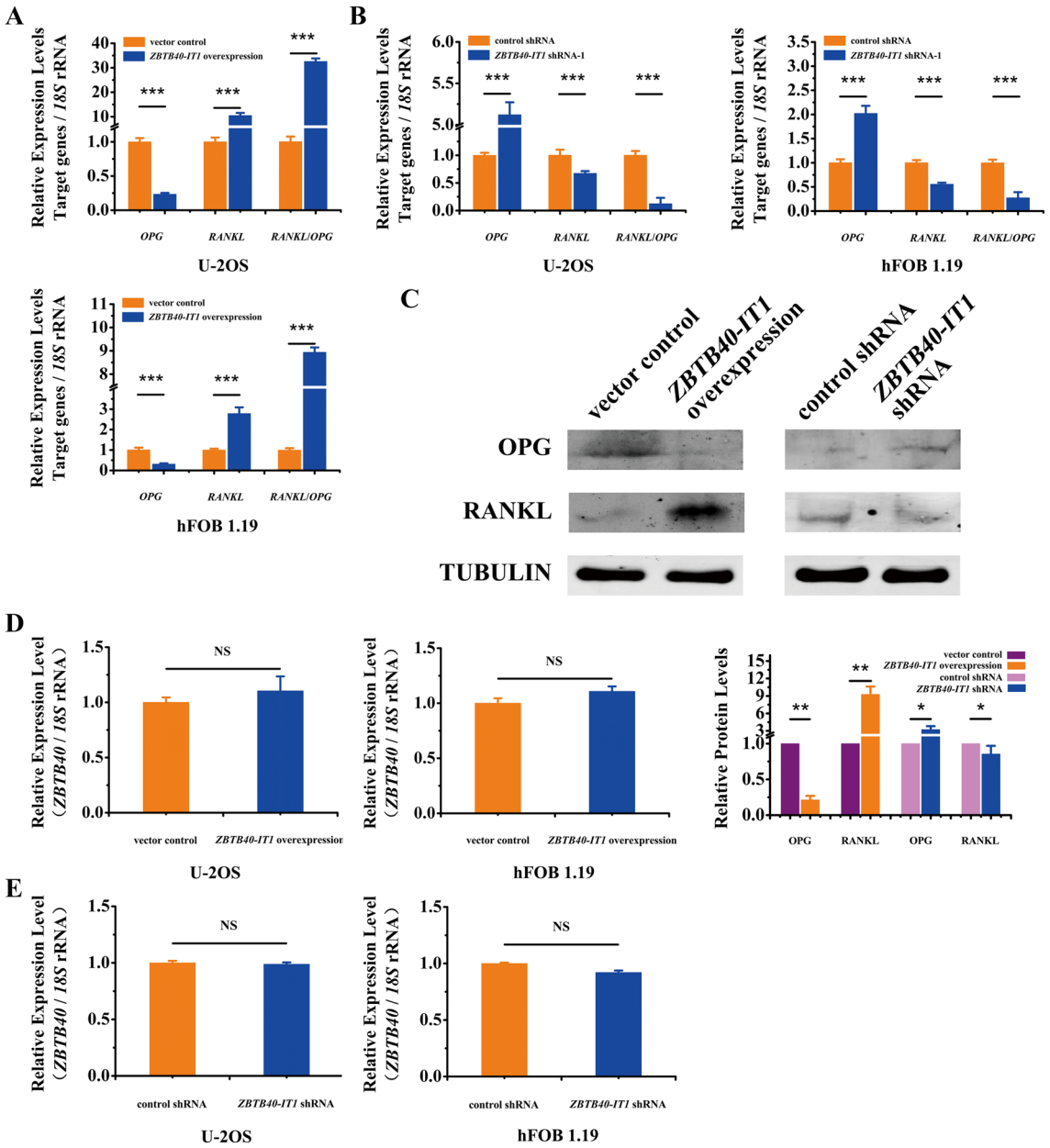

Fig. 2 Effect of LncRNA ZBTB40-IT1 on expression of *ZBTB40* and osteoclastogenesis related genes. Relative expression of *OPG* and *RANKL* in U-2OS and hFOB1.19 cells after *ZBTB40-IT1* overexpression (**a**) or shRNA-mediated knockdown (**b**) as measured by real-time qRT-PCR. **c** Immunoblot analysis of OPG and RANKL with overexpression or shRNA-mediated knockdown of *ZBTB40-IT1* in U-2OS cells and gray-scale analyses of the protein bands. Expression of *ZBTB40* in U-2OS and hFOB1.19 cells after overexpression (**d**) or shRNA-mediated knockdown (**e**) of *ZBTB40-IT1* as measured by real-time qRT-PCR. Error bars show the standard deviation for five technical replicates of a representative experiment. *P* values were calculated by a two-tailed Student's *t* test. $^{**}P < 0.01$, $^{***}P < 0.001$

are designated as 'forward' or 'inverted' based on their orientation with respect to the SNP locations in the reference genome. Site-directed mutagenesis was performed with the Site-Directed Mutagenesis Kit (BS9282, Sangon Biotech, China) according to the manufacturer's instruction. All short hairpin RNA (shRNA) were synthesized and cloned into the pSuper.puro (Invitrogen, USA, VEC-PBS-0008) following the manufacturer's protocol.

The cDNA of CREB1 was amplified by PCR and inserted into p3 × FLAG-CMV-10 (Sigma, St Louis, MO). JUN and FOS cDNAs were cloned into pIRES2-EGFP (Clontech, Palo Alto, CA). DNA segments containing ZBTB40-IT1 genome sequence (3.5-kb) was amplified by PCR using U-2OS cell genomic DNA as templates and inserted into pCMV-MIR vector (OriGene, Rockville, USA). All cloned

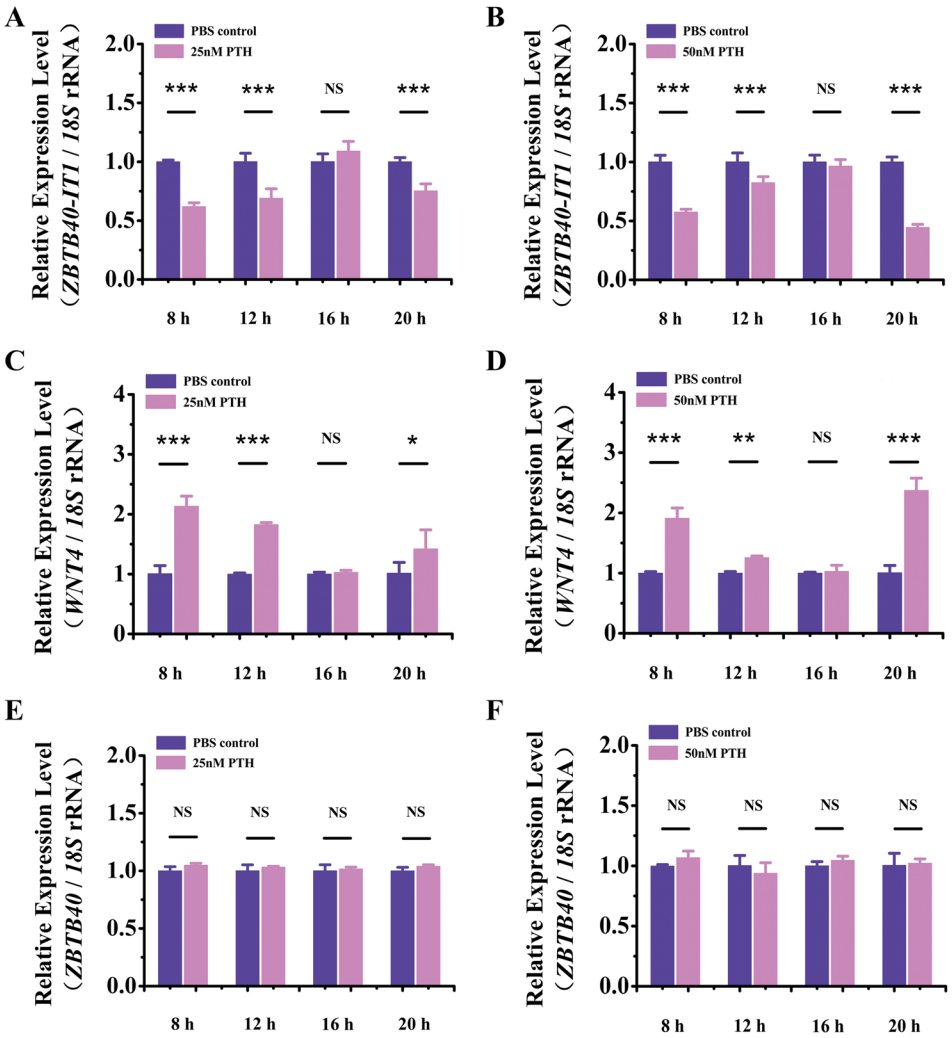

Fig. 3 Response of *ZBTB40-IT1* to PTH treatment in osteoblast-like cell lines. **a, b** *ZBTB40-IT1* downregulation induced by 25 nM or 50 nM PTH (1–34) stimulation for 8 h, 12 h, 16 h and 20 h in U-2OS cells. **c, d** *WNT4* upregulation induced by 25 nM or 50 nM PTH (1–34) stimulation for 8 h, 12 h, 16 h and 20 h in U-2OS cells. E-F. Expression of *ZBTB40* induced by 25 nM or 50 nM PTH (1–34) stimulation for 8 h, 12 h, 16 h and 20 h in U-2OS cells. Error bars show the standard deviation for five technical replicates of a representative experiment. *P* values were calculated by a two-tailed Student's *t* test. $^{**}P < 0.01$, $^{***}P < 0.001$

sequences were verified by sequencing. All primers used were listed in Supplementary Table S1.

Transfection and luciferase reporter assay

U-2OS, Saos-2 and hFOB1.19 cells were transfected using Lipofectamine™ 3000 reagent (Invitrogen, Carlsbad, California, USA) according to the manufacturer's instructions. With regard to HEK293T cells, the transfections were conducted with Neofect™ DNA transfection reagent. The pRL-SV40 vector which is equipped with the Renilla luciferase gene was used as an internal control. After 48 h of transfection, the cells were lysed and luminescence (relative light units) was measured using the Dual-Glo Assay system (Promega, USA, E1910) according to the manufacturer's instructions. $n = 6$ and is representative for three or more independently performed experiments.

RNA extraction, reverse transcription and real-time quantitative PCR

Total RNAs were extracted from the cell lines using TRIzol reagent and the Ultrapure RNA Kit. RNA concentrations were determined by a Nanodrop 1000 (Thermo Scientific, Wilmington, USA). For real-time quantitative reverse transcription (qRT-PCR), first-strand cDNA was synthesized using Superscript III First strand synthesis kit (Life Technologies). Real-time qRT-PCR was conducted in the CFX96 Touch™ Real-Time PCR Detection System (Bio-Rad, USA) with the SYBR Green Mix. Results were analyzed using the comparative Ct method normalizing to a control sample and human *18S* rRNA was used as an internal control. The primers used are listed in Supplemental Table S1.

Western blot analysis

Cells were washed with PBS (pH 7.4) and then lysed in RIPA lysis buffer with freshly added protease inhibitor

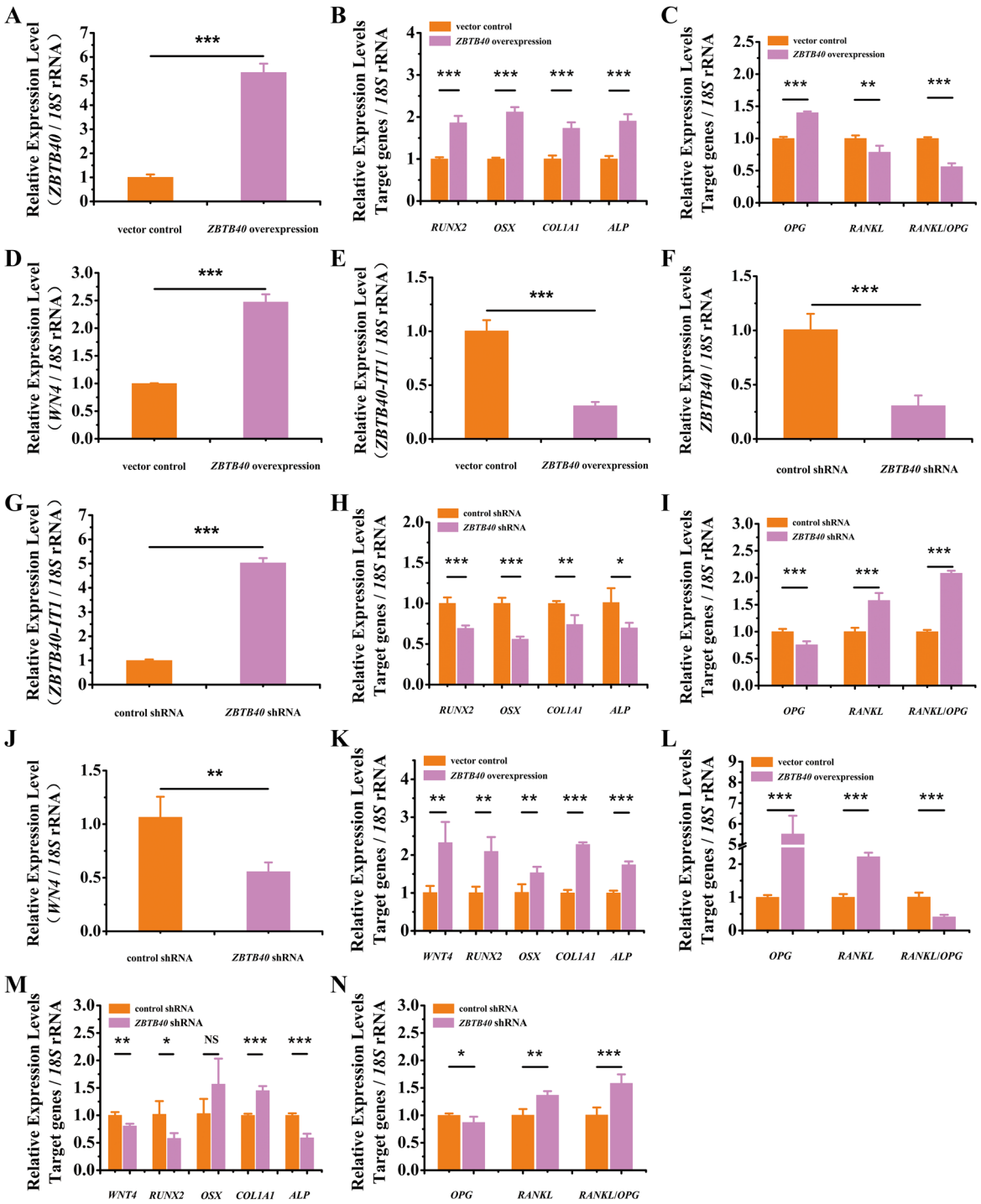

cocktail for 90 min on ice. After centrifugation at 16,000*g* at 4 °C for 30 min, the supernatants were collected and the protein concentration was determined by Pierce BCA Protein Assay Kit. Proteins were separated by SDS-PAGE and then transferred to PVDF membranes. After blocking, the membranes were incubated with primary antibodies overnight at 4 °C and then with Near-Infrared Fluorescent secondary antibodies at room temperature for 4 h. After washing, membranes were scanned on the Odyssey Imaging System and images were analyzed using Image J.

Biotin pull-down assay

Biotin pull-down assays were performed to detect proteins bound to rs6426749 and rs34920465 and the CREB1 or JUN protein present in the pull-down material were detected by

◂**Fig. 4** ZBTB40 promotes osteogenesis and inhibits osteoclastogenesis and the expression of lncRNA ZBTB40-IT1. **a** Upregulation of *ZBTB40* after transfecting *ZBTB40* expression vector in U-2OS. **b** Relative expression of osteogenesis related gene *RUNX2, OSX, COL1A1* and *ALP* with *ZBTB40* overexpression as measured by real-time qRT-PCR. **c** Relative expression of osteoclastogenesis related gene *OPG* and *RANKL* with *ZBTB40* overexpression as measured by real-time qRT-PCR. **d, e** Relative expression of *WNT4* and *ZBTB40-IT1* in U-2OS cells after overexpression of *ZBTB40* as measured by real-time qRT-PCR. **f, g** Expression of *ZBTB40* and *ZBTB40-IT1* after shRNA-mediated knockdown of *ZBTB40* in U-2OS cells as measured by real-time qRT-PCR. **h** Relative expression of osteogenesis related gene *RUNX2, OSX, COL1A1* and *ALP* after shRNA-mediated knockdown of *ZBTB40* as measured by real-time qRT-PCR. **i** Relative expression of osteoclastogenesis related gene *OPG* and *RANKL* after shRNA-mediated knockdown of *ZBTB40* as measured by real-time qRT-PCR. **j** Expression of *WNT4* in U-2OS cells after shRNA-mediated knockdown of *ZBTB40* as measured by real-time qRT-PCR. **k** The effect of *ZBTB40-IT1* overexpression after *ZBTB40* overexpression on the expression of *WNT4* and osteogenesis related gene *RUNX2, OSX, COL1A1* and *ALP* as measured by real-time qRT-PCR. **l** The effect of *ZBTB40-IT1* overexpression after *ZBTB40* overexpression on the expression of osteoclastogenesis related gene *OPG* and *RANKL* as measured by real-time qRT-PCR. **m** The effect of *ZBTB40-IT1* knockdown after *ZBTB40* knockdown on the expression of *WNT4* and osteogenesis related gene *RUNX2, OSX, COL1A1* and *ALP* as measured by real-time qRT-PCR. **n** The effect of *ZBTB40-IT1* knockdown after *ZBTB40* knockdown on the expression of osteoclastogenesis related gene *OPG* and *RANKL* as measured by real-time qRT-PCR. Error bars show the standard deviation for five technical replicates of a representative experiment. *P* values were calculated by a two-tailed Student's *t* test. NS: $P > 0.05$, $^{*}P < 0.05$, $^{**}P < 0.01$, $^{***}P < 0.001$

western blot analysis. Briefly, chemically synthesized oligonucleotides encompassing rs6426749-C or rs6426749-G, rs34920465-A or rs34920465-G (− 20 to + 21 nt) were biotinylated at the 5′-end of the strands and thiol-substituted phosphodiester bonds were used at the 3′-end of the strands to prevent enzymatic cleavage. The sequences are listed in Supplemental Table S1. These sense and anti-sense oligos were annealed and incubated with nuclear extracts from 293T cells with rotation at 4 °C. 4 h after incubation, streptavidin-coupled Sepharose beads (Cell Signaling Technology, #3419) were added to isolate the DNA–protein complex for another 4 h. The beads were washed three times with TGEDN buffer [120 mM Tris-HCl (pH 8.0), 1 mM EDTA, 0.1 M NaCl, 1 mM DTT, 0.1% Triton X-100, 10% glycerol], and bound proteins were eluted with the same buffer supplemented with 0.5% SDS and 1 M NaCl. Eluted proteins were resolved by 10% SDS-PAGE, and proteins pulled down by rs6426749 and rs34920465 were analyzed by immunoblotting with anti-CREB1 and anti-JUN antibody respectively.

Statistical analysis

Data are presented as mean ± SD. Statistical differences between two groups were determined by the two-tailed Student's *t* test. Statistical differences among groups were analyzed by one-way ANOVA followed by Student–Neuman–Keuls' multiple comparisons test. All experiments were performed independently at least three times with similar results, and representative experiments are shown. $P < 0.05$ was considered statistically significant. NS > 0.05, $^{*}P < 0.05$, $^{**}P < 0.01$, $^{***}P < 0.001$.

Results

LncRNA ZBTB40-IT1 inhibites osteogenesis and promotes osteoclastogenesis

To explore the functional role of lncRNA ZBTB40-IT1 in bone metabolism, we performed overexpression and knockdown of *ZBTB40-IT1* in the osteoblast-like U-2OS and hFOB1.19 cells. Previous studies showed that *WNT4* could promote osteoblast differentiation of MSCs (Chang et al. 2007), and increased bone mass through decreased bone resorption and increased bone formation (Yu et al. 2014). We found that overexpression of *ZBTB40-IT1* substantially repressed WNT4 expression at both mRNA and protein levels (Fig. 1a, e), while knockdown of *ZBTB40-IT1* showed an opposite effect (Fig. 1b, e). Moreover, overexpression of *ZBTB40-IT1* inhibited osteogenesis, which was indicated by decreased mRNA level of osteogenic marker genes *RUNX2, OSX, COL1A1* and *ALP* (Fig. 1c) and the protein levels of RUNX2 and OSX (Fig. 1e), while knockdown of *ZBTB40-IT1* increased the mRNA levels of *WNT4, RUNX2, OSX, COL1A1* and *ALP* (Fig. 1d) and protein levels of WNT4, RUNX2 and OSX (Fig. 1e).

Osteoblasts are not only in charge of bone formation but also capable of regulating osteoclast development by secreting RANKL and OPG. OPG is a soluble decoy receptor that can prevent osteoclastogenesis by binding to RANKL with high affinity, potently blocking RANKL through interacting with the osteoclast receptor RANK (Wada et al. 2006). Overexpression of *ZBTB40-IT1* in U-2OS and hFOB1.19 cells resulted in a significant reduction of OPG expression and an increase of RANKL expression at both mRNA and protein levels (Fig. 2a, c). On the contrary, knockdown of *ZBTB40-IT1* displayed opposite effects in osteogenic and osteoclastogenic processes (Fig. 2b, c). However, the expression of *ZBTB40* did not alter in the presence or absence of lncRNA ZBTB40-IT1 (Fig. 2d, e). These results suggested that lncRNA ZBTB40-IT1 played dual roles in both bone formation and bone resorption.

LncRNA ZBTB40-IT1 is responsive to PTH in osteoblast-like cell lines

It is well-known that PTH is a potent stimulator of osteoblastic cell in vitro (Swarthout et al. 2001) and bone resorption and formation in vivo (Dempster et al. 2001; Neer et al.

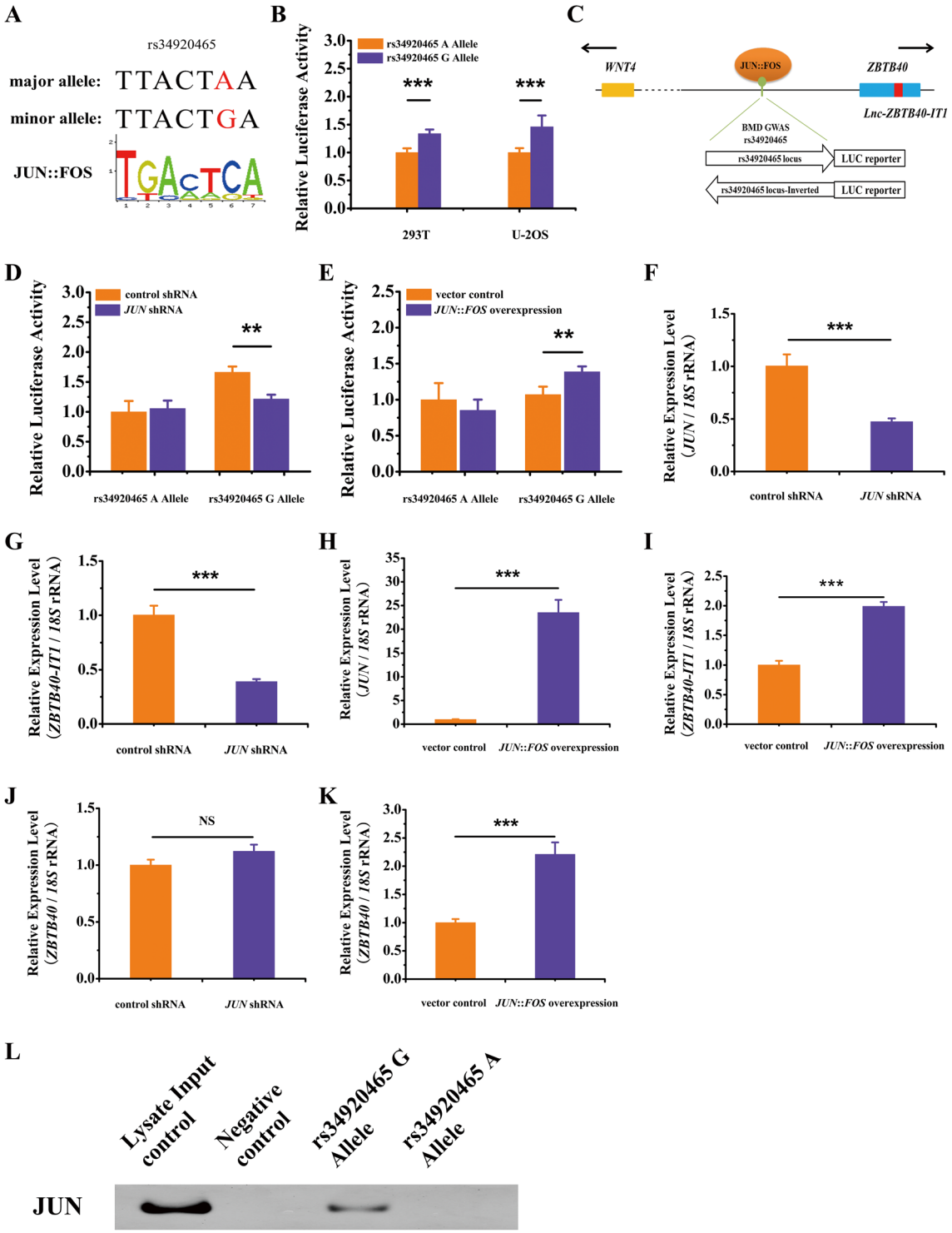

2001). PTH peptides have been clinically used as osteoanabolic therapies for osteoporosis and fracture prevention. Thus, we investigated the effect of PTH treatment on the expression of lncRNA ZBTB40-IT1. The expression level of *ZBTB40-IT1* in U-2OS cells was determined by real-time qRT-PCR. After the treatment with 25 nM and 50 nM PTH (1–34), the expression of lncRNA ZBTB40-IT1 was significantly reduced at 8 h, gradually recovered at 12 h, 16 h, and notably decreased again at 20 h, displaying a strong response to PTH at 8 h and 20 h (Fig. 3a, b). We also found that PTH treatment elevated the expression of *WNT4* at 8 h, 12 h and 20 h (Fig. 3c, d), consistent with previous studies (Bergenstock et al. 2007, 2008). However, PTH

◂**Fig. 5** Rs34920465 G/A alleles differentially bind to JUN::FOS. **a** Motif analysis predicted that JUN::FOS motif binds to the G allele of rs34920465. **b** Luciferase reporter assays using vectors containing the rs34920465 A/G allele in 293T and U-2OS cells. The pGL3-Promoter plasmid (empty) was used as a baseline control. **c** Schematic view of the transcription factor and vectors used in luciferase assays. The yellow box, blue box and red box indicate the *WNT4, ZBTB40* and lncRNA *ZBTB40-IT1* gene respectively; the thin black line indicates the intergenic genomic region; the thick black arrows indicate transcription direction; orange oval indicates the transcription factor JUN::FOS; the hollow arrows represent the fragment direction in the constructs according to the genome. Luciferase reporter assays showing the effect of shRNA-mediated *JUN* knockdown (**d**) or *JUN::FOS* overexpression (**e**) on luciferase activity of rs34920465 A/G alleles in U-2OS cells. *JUN* knockdown mediated by shRNA (**f**) down-regulated *ZBTB40-IT1* expression in Saos-2 cells (**g**) as measured by real-time qRT-PCR. *JUN::FOS* overexpression (**h**) up-regulated *ZBTB40-IT1* expression (**i**) as measured by real-time qRT-PCR. Relative expression of *ZBTB40* in the absence (**j**) or presence (**k**) of *JUN::FOS* as measured by real-time qRT-PCR. **l** HEK293T cell lysates were incubated with 5′ end biotin-labeled rs34920465 G/A alleles and negative control sequences (JUN::FOS binding element deletion) for biotin pull-down assay, followed by western blot analysis. Luciferase signal was normalized to Renilla signal. Error bars show the standard deviation for five technical replicates of a representative experiment. *P* values were calculated by a two-tailed Student's *t* test. $^{**}P < 0.01$, $^{***}P < 0.001$

treatment did not influence the expression of the *ZBTB40* gene (Fig. 3e, f).

ZBTB40 promotes osteogenesis and inhibits osteoclastogenesis and the expression of lncRNA ZBTB40-IT1

To explore the functional role of the *ZBTB40* gene in bone metabolism, overexpression and knockdown of *ZBTB40* were performed in U-2OS cells. Overexpression of *ZBTB40* (Fig. 4a) elevated the mRNA levels of *RUNX2, OSX, COL1A1, ALP*, and *OPG* (Fig. 4b, c), *WNT4* (Fig. 4d), and reduced levels of lncRNA *ZBTB40-IT1* (Fig. 4e) and *RANKL* (Fig. 4c), while knockdown of *ZBTB40* (Fig. 4f) elevated the expression levels of *ZBTB40-IT1* (Fig. 4g) and *RANKL* (Fig. 4i), and reduced mRNA levels of *RUNX2, OSX, COL1A1, ALP, OPG*, and *WNT4* (Fig. 4h–j). These results suggested that *ZBTB40* can promote osteogenesis and inhibit osteoclastogenesis and the expression of lncRNA ZBTB40-IT1. Interestingly, overexpression of *ZBTB40-IT1* had no effect on the downstream effect of *ZBTB40* on marker genes except for *RANKL* (Fig. 4b, c, k, l), and knockdown of *ZBTB40-IT1* had no effect on the downstream effect of *ZBTB40* on marker genes except for *COL1A1* (Fig. 4h, i, m, n), indicating that the regulatory role of *ZBTB40* may be independent of *ZBTB40-IT1*, and that further functional assays are needed to elucidate the precise molecular mechanisms underlying these two genes.

The rs34920465 regulates the expression of endogenous lncRNA *ZBTB40-IT1* and *ZBTB40* genes by differential binding of JUN::FOS

Data from the dbSNP database showed that the G allele of rs34920465 is the ancestral and global minor allele with a frequency of 0.2746. An investigation in the JASPAR database indicated that the rs34920465 is located within the core consensus binding site of the transcription factor JUN::FOS and the G allele is predicted to bind JUN::FOS (Fig. 5a). To evaluate whether rs34920465 has significant intrinsic transcriptional regulatory functions, we performed an in vitro luciferase-based reporter assay. The 3.5-kb DNA fragments with rs34920465 G/A alleles in the middle region showed differential allelic enhancer activity in both U-2OS and HEK293T cell lines. Compared with the major rs34920465-A allele, the minor rs34920465-G allele showed a 1.46-fold and a 1.33-fold increase of transcriptional activity in U-2OS and HEK293T cells, respectively (Fig. 5b).

To determine whether the differential allelic enhancer activities were actually mediated by JUN::FOS (Fig. 5c), we assessed the impacts of *JUN::FOS* knockdown achieved by *JUN* shRNA and *JUN* and *FOS* overexpression on transcriptional activities of rs34920465 alleles. In the presence of *JUN* shRNA, the rs34920465-G showed a 30% significant decrease in luciferase activity in U-2OS cells, while the rs34920465-A did not respond (Fig. 5d). In contrast, cotransfection with the *JUN* and *FOS* overexpression vectors

Table 1 Genotypes of cell lines at relevant SNPs

SNP	Gene region	Binding factor	Cell line	Genotype[a,b]
rs34920465	*WNT4/ZBTB40* upstream	JUN::FOS	U-2OS	a/a
			Saos-2	**G**/a
			293T	a/a
			hFOB1.19	a/a
rs6426749	*WNT4/ZBTB40* upstream	CREB1	U-2OS	g/**C**
			Saos-2	**C/C**
			293T	g/g
			hFOB1.19	g/g

[a]Capital letter indicates the major allele and small letter indicates the minor allele

[b]Bold letter denotes the binding allele

resulted in an increase of luciferase activity of rs34920465 in a G allele-preferential manner in the U-2OS cell line (Fig. 5e).

To determine whether JUN::FOS affects endogenous *ZBTB40-IT1* and *ZBTB40* expression, we respectively transfected *JUN* shRNA vector and *JUN* and *FOS* overexpression vector in the Saos-2 cells carrying rs34920465 G/A alleles (Table 1). The expression level of *ZBTB40-IT1* was decreased in the absence of *JUN* (Fig. 5f, g), and increased in the presence of *JUN* and *FOS* (Fig. 5h, i). Notably, knockdown of *JUN* did not alter the expression of *ZBTB40* (Fig. 5j), while cotransfection with the *JUN* and *FOS* overexpression vectors elevated *ZBTB40* expression level (Fig. 5k).

To assess whether rs34920465 G/A alleles differentially affect JUN::FOS-DNA binding in vitro, biotin-labeled probes of about 42 bp surrounding the rs34920465-G/A were incubated with nuclear lysate from HEK293T and subjected to biotin pull-down assays. DNA-JUN::FOS complex was observed for the G allele containing probe but not for the A allele containing probe, suggesting differential JUN::FOS binding dependent on the specific rs34920465 G allele (Fig. 5l).

Fig. 7 rs6426749 G/C alleles modulate CREB1 binding. **a** Motif analysis predicted that CREB1 likely binds to G allele of rs6426749. **b** Luciferase reporter assays using vectors containing the rs6426749 G/C allele in 293T and U-2OS cells. The pGL3-Promoter plasmid (empty) was used as a baseline control. **c** Schematic view of the transcription factor and vectors used in luciferase assays. The yellow box, blue box and red box indicate the *WNT4, ZBTB40* and lncRNA *ZBTB40-IT1* gene respectively; the thin black line indicates the intergenic genomic region; the thick black arrows indicate transcription direction; faint red oval indicates the transcription factor CREB1; the hollow arrows represent the fragment direction in the constructs according to the genome. Luciferase reporter assays showing the effect of shRNA-mediated knockdown (**d**) or overexpression (**e**) of *CREB1* on luciferase activity of rs34920465 G/C alleles in U-2OS cells. **f, g** shRNA-mediated *CREB1* knockdown reduced *ZBTB40-IT1* expression in U-2OS cells as measured by real-time qRT-PCR. **h, i** *CREB1* overexpression increased *ZBTB40-IT1* expression as measured by real-time qRT-PCR. Relative expression of *ZBTB40* in the absence (**j**) or presence (**k**) of *CREB1* as measured by real-time qRT-PCR. **l** HEK293T cell lysates were incubated with 5′ end biotin-labeled rs6426749 G/C alleles and negative control sequences (CREB1 binding element deletion) for biotin pull-down assay, followed by western blot analysis. Luciferase signal was normalized to Renilla signal. Error bars show the standard deviation for five technical replicates of a representative experiment. *P* values were calculated by a two-tailed Student's *t* test. $^{**}P<0.01$, $^{***}P<0.001$

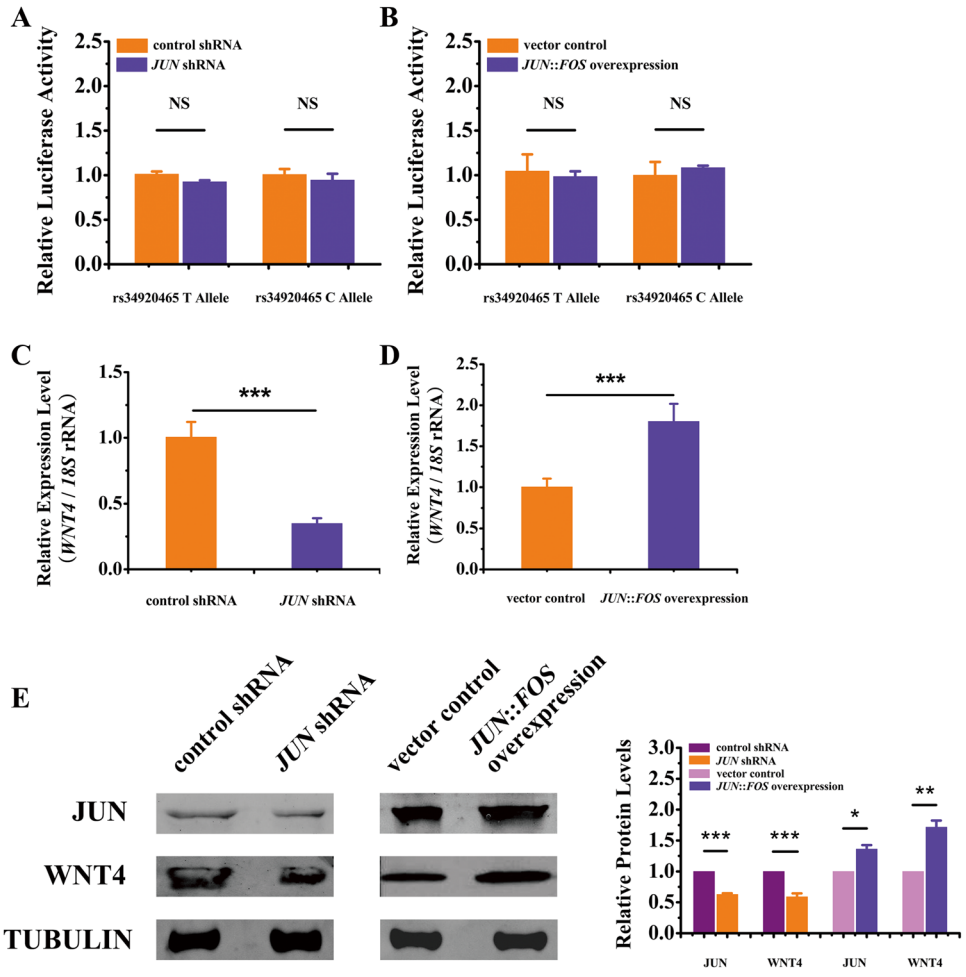

Fig. 6 Effect of JUN::FOS on the expression of endogenous *ZBTB40-IT1, ZBTB40 and WNT4* genes in rs34920465 G/A heterozygous Saos-2 cells. Luciferase reporter assays showing the effect of shRNA-mediated *JUN* knockdown (**a**) or JUN::FOS overexpression (**b**) on luciferase activity of rs34920465 T/C (fragment inverted orientation) alleles in U-2OS cells. Relative expression of *WNT4* in the absence (**c**) or presence (**d**) of *JUN::FOS* as measured by real-time qRT-PCR. **e** Immunoblot analysis of JUN and WNT4 after shRNA-mediated *JUN* knockdown or *JUN::FOS* overexpression in Saos-2 cells and gray-scale analyses of the protein bands. Error bars show the standard deviation for five technical replicates of a representative experiment. *P* values were calculated by a two-tailed Student's *t* test. $^{**}P<0.01$, $^{***}P<0.001$

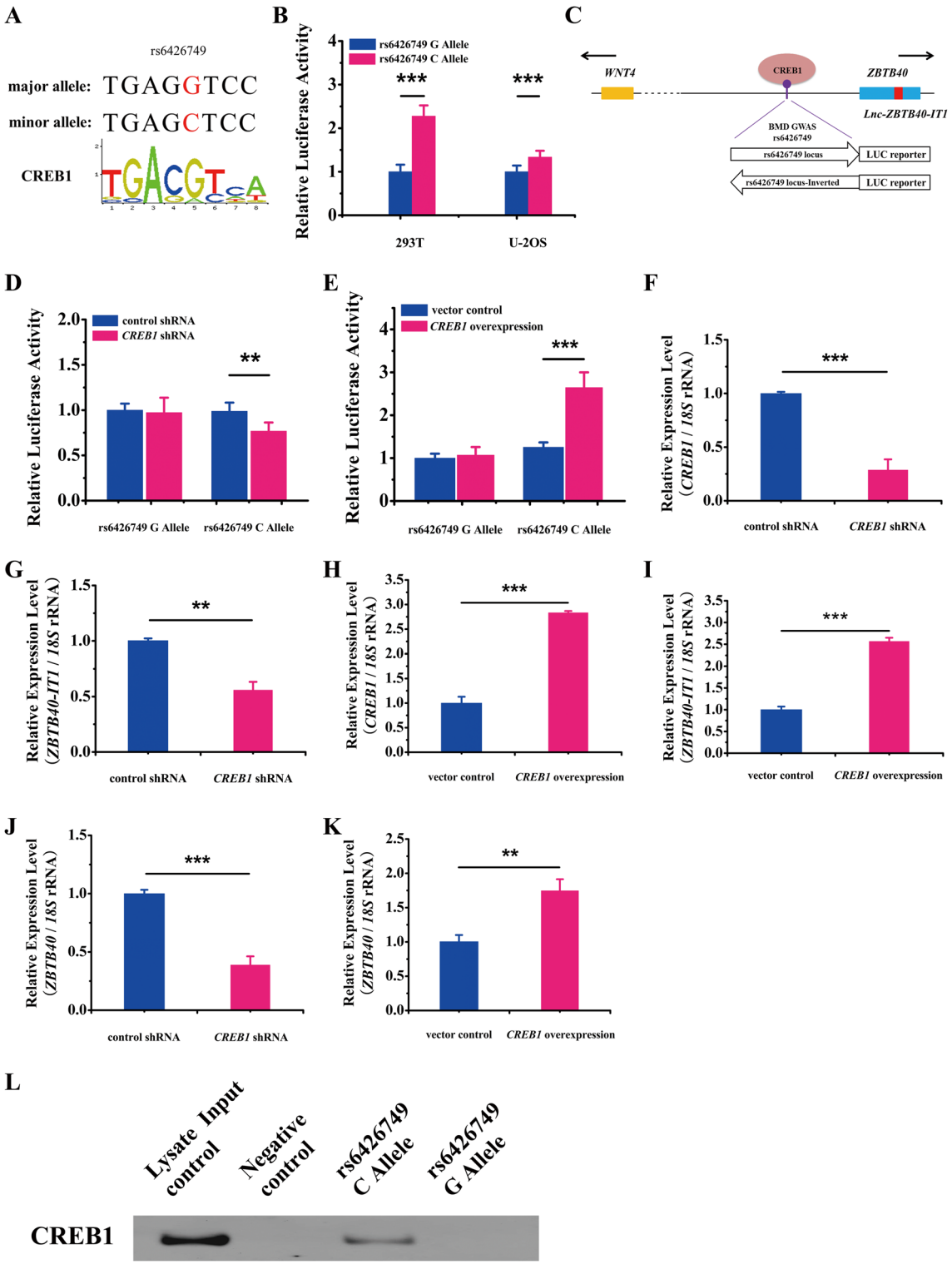

SNP rs34920465 is located between *ZBTB40* and *WNT4*, which are transcribed in opposite directions. 1p36 is an evolutionarily conserved region (Zhang et al. 1999). Evidences showed that many conserved intergenic or upstream region of genes functioned as motifs or modules that possess bidirectional transcription activity (Kurihara et al. 2014; Liu et al. 2016). To explore whether rs34920465 also has transcription enhancer activity for *WNT4*, a 3.5-kb inverted fragment with rs34920465 T/C alleles in the middle region was respectively inserted into luciferase reporter vector (Fig. 5c), and was co-transfected with *JUN* shRNA or *JUN* and *FOS* overexpression vectors into U-2OS cells. Neither rs34920465-T nor

rs34920465-C showed differences in luciferase activity in the presence of *JUN* shRNA or *JUN* and *FOS* overexpression vector, suggesting that rs34920465 has no transcription enhancer activity for *WNT4* (Fig. 6a, b). Interestingly, knockdown of JUN downregulated WNT4 expression at both mRNA and protein levels (Fig. 6c, e), while cotransfection with the JUN and FOS overexpression vectors upregulated WNT4 expression at both mRNA and protein levels (Fig. 6d, e).

The rs6426749 regulates the expression of endogenous lncRNA *ZBTB40-IT1* and *ZBTB40* genes by differential binding of CREB1

The risk C allele of rs6426749 is the ancestral and global minor allele with a frequency of 0.2147. Computational analysis based on the JASPAR database 2016 showed that the rs6426749 is located in the binding sequence and the G allele is predicted to bind CREB1 (Fig. 7a). To examine whether rs6426749 has significant intrinsic transcriptional regulatory functions, we cloned 3.4-kb rs6426749 locus with the G/C alleles, and inserted into a luciferase reporter vector, and carried out the luciferase-based reporter assay in U-2OS and HEK293T cell lines. The rs6426749-C allele showed significantly higher luciferase activity than the rs6426749-G allele in both U-2OS and HEK293T cell lines (Fig. 7b). The most prominent difference was observed in HEK293T cells with a 2.27-fold discrepancy.

To investigate whether the differential allelic transcriptional activities were actually mediated by CREB1 (Fig. 7c), we next sought to determine the impacts of CREB1 knockdown achieved by *CREB1* shRNA and *CREB1* overexpression on transcriptional activities of rs6426749 alleles. In the presence of *CREB1* shRNA, the rs6426749-C exhibited a 22.2% significantly decreased transcriptional activity in the U-2OS cell (Fig. 7d), whereas the rs6426749-G allele had no response (Fig. 7d). In contract, cotransfection with the *CREB1* overexpression vector resulted in a dramatic increase of transcriptional activities of rs6426749 in a C allele-preferential manner in U-2OS cells (Fig. 7e).

To further investigate the effects of CREB1 on endogenous *ZBTB40-IT1* and *ZBTB40* expression, we employed a RNA interference vector for CREB1 and constructed a CREB1 expressing plasmid based on the p3xFLAG-CMV-10 vector. In heterozygous U-2OS cells carrying rs6426749 G/C (Table 1), *CREB1* shRNA treatment significantly reduced the *ZBTB40-IT1* expression (Fig. 7f, g), while overexpression of *CREB1* (Fig. 7h) led to increased *ZBTB40-IT1* expression (Fig. 7i). Notably, knockdown of *CREB1* decreased the expression of *ZBTB40* (Fig. 7j), while *ZBTB40* expression level was elevated in the present of *CREB1* overexpression vector (Fig. 7k).

To assess whether rs6426749 G/C alleles differentially affect CREB1-DNA binding in vitro, biotin-labeled probes of about 42 bp surrounding the rs6426749-C/G alleles were incubated with nuclear lysate from HEK293T and subjected to biotin pull-down assays. DNA–CREB1 complex was observed for the C allele containing probe but not for the G allele containing probe, suggesting differential CREB1 binding dependent on the specific rs6426749 C allele (Fig. 7l).

Similar to rs34920465, to explore whether rs6426749 also has transcription enhancer activity for the *WNT4* gene, luciferase reporter vector equipped with rs6426749 G/C allele 3.4-kb inverted fragment (Fig. 7c) or not was co-transfected with *CREB1* shRNA or *CREB1* overexpression vector into U-2OS cells, respectively. Luciferase activity of the rs6426749-C or rs6426749-G showed no differences in the presence of *CREB1* shRNA or *CREB1* overexpression vector (Fig. 8a, b), suggesting that rs6426749 has no transcription enhancer activity for *WNT4*. However, knockdown of CREB1 reduced WNT4 expression at both mRNA and protein levels (Fig. 8c, e), while transfection with the CREB1 overexpression vector up-regulated WNT4 expression at both mRNA and protein levels (Fig. 8d, e).

Collectively, these results indicated that CREB1 played a positive modulatory role in the expression of endogenous *ZBTB40-IT1* and *ZBTB40* genes. Interestingly, although rs6426749 has no transcription enhancer activity for the *WNT4* gene, *WNT4* expression level was altered in the presence of *CREB1* shRNA or *CREB1* overexpression vector.

Discussion

LncRNAs play the important regulatory roles in disease development including osteoporosis. The FANTOM5 Project (Hon et al. 2017) demonstrated that almost 20,000 potential functional lncRNAs overlapped with trait- or eQTL-associated SNPs. A few lncRNAs related to diseases have been identified and well-characterized, including PCAT19 (Hua et al. 2018), PCAT1 (Guo et al. 2016), LINC00339 (Chen et al. 2018; Powell et al. 2016), LINC00673 (Zheng et al. 2016), PTCSC2 (Wang et al. 2017a, b). LncRNA ZBTB40-IT1 is ubiquitously expressed in various tissues and its function in bone metabolism is unknown. Here we showed that *ZBTB40-IT1* could suppress osteogenesis and promote osteoclastogenesis by downregulating the expression of *WNT4, RUNX2, OSX, ALP, COL1A1*, and reducing the *RANKL*/*OPG* ratio. PTH, the only FDA-approved anabolic agent for osteoporosis treatment, plays a vital role in bone resorption and bone formation via maintaining calcium homeostasis and regulating bone metabolism. Here we discovered that PTH treatment significantly reduced the *ZBTB40-IT1* expression and did not alter the *ZBTB40* expression, further supporting the role of lncRNA ZBTB40-IT1 in osteoporosis.

Multiple genome wide analysis discovered that intergenic SNPs rs34920465 and rs6426749 were associated with BMDs for the lumbar spine, hip and femoral neck (Park et al. 2014; Rivadeneira et al. 2009; Zhang et al. 2014). Here we demonstrated that JUN::FOS and CREB1 could respectively bind to rs34920465-G and rs6426749-C alleles to elevate the expression of *ZBTB40* and lncRNA ZBTB40-IT1. JUN::FOS and CREB1 are two crucial stimulators of RANKL-RANK signaling in osteoclast differentiation and maturation (Ikeda et al. 2004; Sato et al. 2006). A recent study showed that rs6426749 can bind transcription factor TFAP2A and act as a distal allele-specific enhancer modulating the expression of *LINC00339* via long-range chromatin loop formation (Chen et al. 2018). Thus, osteoporosis risk SNP rs6426749 may be a pleiotropic locus that could bind multiple transcription factors and regulates the expression of multiple bone metabolism related genes including *LINC00339, ZBTB40-IT1, CDC42* and *ZBTB40*, which all contribute to osteoporosis pathophysiology.

WNT4 is a prototypical ligand for the noncanonical WNT pathway, and could promote osteoblast differentiation of MSCs (Chang et al. 2007). Overexpression of *WNT4* in osteoblasts resulted in increased bone mass due to a combination of decreased bone resorption and increased bone formation, and inhibited osteoclast differentiation via noncanonical WNT signaling (Chang et al. 2007). WNT4 attenuated bone loss in osteoporosis and skeletal aging mouse models (Yu et al. 2014). Data from the GTEx (GTEx Consortium 2015) showed that SNPs rs34920465 and rs6426749 were the eQTL of *WNT4*. The SNP-eQTL analyses found that rs6426749 [G] was correlated with reduced *WNT4* expression in osteoblast (Estrada et al. 2012). However, we found that rs6426749 has no transcription enhancer activity for the *WNT4* gene. Interestingly, the upregulation of *ZBTB40-IT1* can significantly decrease the expression of *WNT4* in osteoblast-like cells. Therefore, it is likely that rs6426749 was correlated with reduced *WNT4* expression through the regulation of *ZBTB40-IT1*. Future investigations are warranted to elucidate the precise molecular mechanisms.

There are certain limitations in this study. First, we illustrated the functionality of SNPs rs34920465 and rs6426749, *ZBTB40* and lncRNA ZBTB40-IT1 in vitro

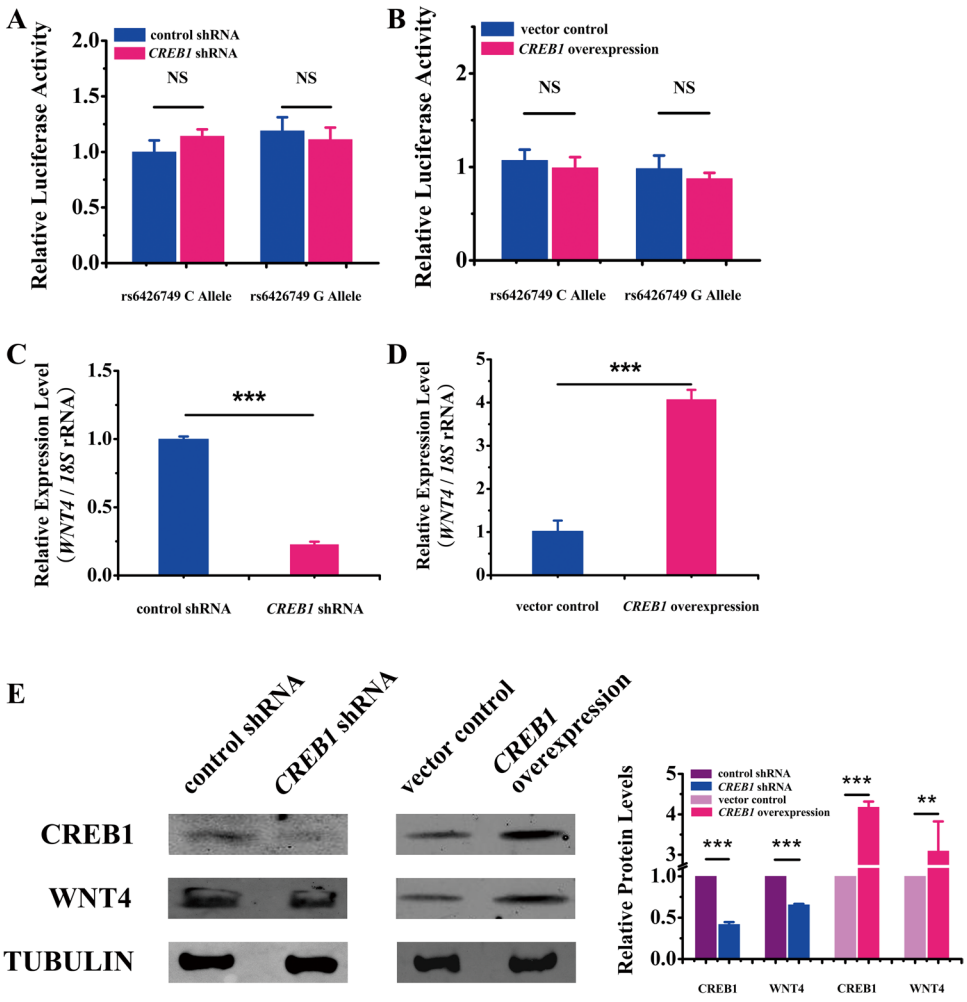

Fig. 8 Effect of CREB1 on the expression of endogenous *ZBTB40-IT1, ZBTB40* and *WNT4* genes in rs6426749 G/C heterozygous U-2OS cells. Luciferase reporter assays showing the effect of shRNA-mediated knockdown (**a**) or overexpression (**b**) of *CREB1* on luciferase activity of rs6426749 C/G (fragment inverted orientation) alleles in U-2OS cells. Relative expression of *WNT4* in the absence (**c**) or presence (**d**) of *CREB1* as measured by real-time qRT-PCR. **e** Immunoblot analysis of CREB1 and WNT4 after shRNA-mediated *CREB1* knockdown or *CREB1* overexpression in U-2OS cells and gray-scale analyses of the protein bands. Error bars show the standard deviation for five technical replicates of a representative experiment. *P* values were calculated by a two-tailed Student's *t* test. $^{**}P < 0.01$, $^{***}P < 0.001$

and lacked the relevant experimental validation in vivo. Second, it is worth noting that our regulatory model could not exclude the contribution of other genetic variants and other binding sites of transcription factors, but instead highlights the results of the study at hand. Finally, our study highlights the regulatory effect of noncoding SNPs rs34920465 and rs6426749 on osteoporosis through lncRNA ZBTB40-IT1. Further functional studies are warranted to investigate the detailed molecular mechanism of ZBTB40-IT1 action.

In summary, we demonstrated that lncRNA ZBTB40-IT1 inhibits osteogenesis and promotes osteoclastogenesis by regulating the expression of a subset of bone metabolism related genes, whereas the *ZBTB40* gene has opposite functional roles. SNPs rs34920465 and rs6426749 regulated the expression of *ZBTB40* and *ZBTB40-IT1* via recruiting transcription factors JUN::FOS and CREB1 respectively in allele-specific manner. Our study provides a potential mechanistic basis for SNPs rs34920465 and rs6426749 with target genes *ZBTB40* and *ZBTB40-IT1* at 1p36 locus.

Acknowledgements This work was supported by the National Natural Science Foundation of China (nos. 31371275 and 30971635) and self-determined research fund of CCNU from the basic research and operation of MOE (CCNU18ZDPY05).

References

Aizawa R, Yamada A, Suzuki D, Iimura T, Kassai H, Harada T, Tsukasaki M, Yamamoto G, Tachikawa T, Nakao K, Yamamoto M, Yamaguchi A, Aiba A, Kamijo R (2012) Cdc42 is required for chondrogenesis and inter-digital programmed cell death during limb development. Mech Dev 129:38–50. https://doi.org/10.1016/j.mod.2012.02.002

Bergenstock MK, Partridge NC (2007) Parathyroid hormone stimulation of noncanonical Wnt signaling in bone. Ann N Y Acad Sci 1116:354–359. https://doi.org/10.1196/annals.1402.047

Bergenstock MK, Partridge NC (2008) Parathyroid hormone (PTH) regulation of non-canonical Wnt-4: a stimulator of differentiation in osteoblasts and bone marrow stromal stem cells. Faseb J 22: 646–649. https://doi.org/10.1096/fasebj.22.1_supplement.646.9

Chang J, Sonoyama W, Wang Z, Jin Q, Zhang C, Krebsbach PH, Giannobile W, Shi S, Wang CY (2007) Noncanonical Wnt-4 signaling enhances bone regeneration of mesenchymal stem cells in craniofacial defects through activation of p38 MAPK. J Biol Chem 282: 30938–30948. https://doi.org/10.1074/jbc.M702391200

Chen XF, Zhu DL, Yang M, Hu WX, Duan YY, Lu BJ, Rong Y, Dong SS, Hao RH, Chen JB, Chen YX, Yao S, Thynn HN, Guo Y, Yang TL (2018) An osteoporosis risk SNP at 1p36.12 acts as an allele-specific enhancer to modulate LINC00339 expression via long-range loop formation. Am J Hum Genet 102:776–793. https://doi.org/10.1016/j.ajhg.2018.03.001

Dempster DW, Cosman F, Kurland ES, Zhou H, Nieves J, Woelfert L, Shane E, Plavetić K, Müller R, Bilezikian J, Lindsay R (2001) Effects of daily treatment with parathyroid hormone on bone microarchitecture and turnover in patients with osteoporosis: a paired biopsy study. J Bone Miner Res 16:1846–1853. https://doi.org/10.1359/jbmr.2001.16.10.1846

Devoto M, Shimoya K, Caminis J, Ott J, Tenenhouse A, Whyte MP, Sereda L, Hall S, Considine E, Williams CJ, Tromp G, Kuivaniemi H, Ala-Kokko L, Prockop DJ, Spotila LD (1998) First-stage autosomal genome screen in extended pedigrees suggests genes predisposing to low bone mineral density on chromosomes 1p, 2p and 4q. Eur J Hum Genet 6:151–157. https://doi.org/10.1038/sj.ejhg.5200169

Devoto M, Specchia C, Li HH, Caminis J, Tenenhouse A, Rodriguez H, Spotila LD (2001) Variance component linkage analysis indicates a QTL for femoral neck bone mineral density on chromosomes 1p36. Hum Mol Genet 10:2447–2452. https://doi.org/10.1093/hmg/10.21.2447

Estrada K, Styrkarsdottir U, Evangelou E, Hsu YH, Duncan EL, Ntzani EE, Oei L, Albagha OM, Amin N, Kemp JP, Koller DL, Li G, Liu CT, Minster RL, Moayyeri A, Vandenput L, Willner D, Xiao SM, Yerges-Armstrong LM,Zheng HF, Alonso N, Eriksson J, Kammerer CM, Kaptoge SK, Leo PJ, Thorleifsson G, Wilson SG, Wilson JF, Aalto V, Alen M, Aragaki AK, Aspelund T, Center JR, Dailiana Z, Duggan DJ, Garcia M, Garcia-Giralt N, Giroux S, Hallmans G, Hocking LJ, Husted LB, Jameson KA, Khusainova R, Kim GS, Kooperberg C, Koromila T, Kruk M, Laaksonen M, Lacroix AZ,Lee SH, Leung PC, Lewis JR, Masi L, Mencej-Bedrac S, Nguyen TV, Nogues X, Patel MS,Prezelj J, Rose L.M, Scollen S, Siggeirsdottir K, Smith AV, Svensson O, Trompet S,Trummer O, van Schoor NM, Woo J, Zhu K, Balcells S, Brandi ML, Buckley BM, Cheng S,Christiansen C, Cooper C, Dedoussis G, Ford I, Frost M, Goltzman D, González-Macías J, Kähönen M, Karlsson M, Khusnutdinova E, Koh JM, Kollia P, Langdahl BL, Leslie WD,Lips P, Ljunggren Ö, Lorenc RS, Marc J, Mellström D, Obermayer-Pietsch B, Olmos JM, Pettersson-Kymmer U, Reid DM, Riancho JA, Ridker PM, Rousseau F, Slagboom PE, Tang NL, Urreizti R, Van Hul W, Viikari J, Zarrabeitia MT, Aulchenko YS, Castano-Betancourt M, Grundberg E, Herrera L, Ingvarsson T, Johannsdottir H, Kwan T, Li R, Luben R, Medina-Gómez C, Palsson, ST, Reppe S, Rotter JI, Sigurdsson G, van Meurs JB, Verlaan D, Williams FM, Wood AR, Zhou Y, Gautvik KM,Pastinen T, Raychaudhuri S, Cauley JA, Chasman DI, Clark GR, Cummings SR, Danoy P,Dennison EM, Eastell R, Eisman, JA, Gudnason V, Hofman A, Jackson RD, Jones G, Jukema JW, Khaw KT, Lehtimäki T, Liu Y, Lorentzon M, McCloskey E, Mitchell BD, Nandakumar K, Nicholson GC, Oostra BA, Peacock M, Pols HA, Prince RL, Raitakari O, Reid IR, Robbins J, Sambrook PN, Sham PC, Shuldiner AR,Tylavsky FA, van Duijn CM, Wareham NJ, Cupples LA, Econs MJ, Evans DM, Harris TB,Kung AW, Psaty BM, Reeve J, Spector TD, Streeten EA, Zillikens MC, Thorsteinsdottir U, Ohlsson C, Karasik D, Richards JB, Brown MA, Stefansson K, Uitterlinden AG, Ralston SH, Ioannidis JP, Kiel DP, Rivadeneira F (2012) Genome-wide meta-analysis identifies 56 bone mineral density loci and reveals 14 loci associated with risk of fracture. Nat Genet 44: 491–501. https://doi.org/10.1038/ng.2249

Greenblatt MB, Shim JH, Glimcher LH (2013) Mitogen-activated protein kinase pathways in osteoblasts. Annu Rev Cell Dev Biol 29:63–79. https://doi.org/10.1146/annurev-cellbio-101512-122347

GTEx Consortium Human Genomics (2015) The genotype-tissue expression (GTEx) pilot analysis: multi-tissue gene regulation in humans. Science 348: 648–660. https://doi.org/10.1126/science.1262110

Guo H, Ahmed M, Zhang F, Yao CQ, Li S, Liang Y, Hua J, Soares F, Sun Y, Langstein J, Li Y, Poon C, Bailey SD, Desai K, Fei T, Li Q, Sendorek DH, Fraser M, Prensner JR, Pugh TJ, Pomerantz M, Bristow RG, Lupien M, Feng FY, Boutros PC, Freedman ML, Walsh MJ, He HH (2016) Modulation of long noncoding RNAs by risk SNPs underlying genetic predispositions to prostate cancer. Nat Genet 48:1142–1150. https://doi.org/10.1038/ng.3637

Hon CC, Ramilowski JA, Harshbarger J, Bertin N, Rackham OJ, Gough J, Denisenko E, Schmeier S, Poulsen TM, Severin J, Lizio M, Kawaji H, Kasukawa T, Itoh M, Burroughs AM, Noma S, Djebali S, Alam T, Medvedeva YA, Testa AC, Lipovich L, Yip CW, Abugessaisa I, Mendez M, Hasegawa A, Tang D, Lassmann T, Heutink P, Babina M, Wells CA, Kojima S, Nakamura Y, Suzuki H, Daub CO, de Hoon MJ, Arner E, Hayashizaki Y, Carninci P, Forrest AR (2017) An atlas of human long non-coding RNAs with accurate 5′ ends. Nature 543:199–204. https://doi.org/10.1038/nature21374

Hua JT, Ahmed M, Guo H, Zhang Y, Chen S, Soares F, Lu J, Zhou S, Wang M, Li H, Larson NB, McDonnell SK, Patel PS, Liang Y, Yao CQ, van der Kwast T, Lupien M, Feng FY, Zoubeidi A, Tsao MS, Thibodeau SN, Boutros PC, He HH (2018) Risk SNP-mediated promoter-enhancer switching drives prostate cancer through lncRNA PCAT19. Cell 174: 564–575. https://doi.org/10.1016/j.cell.2018.06.014

Huang Y, Zheng Y, Jia L, Li W (2015) Long noncoding RNA H19 promotes osteoblast differentiation via TGF-β1/Smad3/HDAC signaling pathway by deriving miR-675. Stem Cells 33:3481–3492. https://doi.org/10.1002/stem.2225

Ikeda F, Nishimura R, Matsubara T, Tanaka S, Inoue J, Reddy SV, Hata K, Yamashita K, Hiraga T, Watanabe T, Kukita T, Yoshioka K, Rao A, Yoneda T (2004) Critical roles of c-Jun signaling in regulation of NFAT family and RANKL-regulated osteoclast differentiation. J Clin Investig 114:475–584. https://doi.org/10.1172/JCI19657

Ito Y, Teitelbaum SL, Zou W, Zheng Y, Johnson JF, Chappel J, Ross FP, Zhao H (2010) Cdc42 regulates bone modeling and remodeling in mice by modulating RANKL/M-CSF signaling and osteoclast polarization. J Clin Investig 120:1981–1993. https://doi.org/10.1172/JCI39650

Kemp JP, Medina-Gomez C, Estrada K, St Pourcain B, Heppe DH, Warrington NM, Oei L, Ring SM, Kruithof CJ, Timpson NJ, Wolber LE, Reppe S, Gautvik K, Grundberg E, Ge B, van der Eerden B, van de Peppel J, Hibbs MA, Ackert-Bicknell CL, Choi K, Koller DL, Econs MJ, Williams FM, Foroud T, Zillikens MC, Ohlsson C, Hofman A, Uitterlinden AG, Davey Smith G, Jaddoe VW, Tobias JH, Rivadeneira F, Evans DM (2014) Phenotypic dissection of bone mineral density reveals skeletal site specificity and facilitates the identification of novel loci in the genetic regulation of bone mass attainment. PLoS Genet 10:e1004423. https://doi.org/10.1371/journal.pgen.1004423

Kemp JP, Morris JA, Medina-Gomez C, Forgetta V, Warrington NM, Youlten SE, Zheng J, Gregson CL, Grundberg E, Trajanoska K, Logan JG, Pollard AS, Sparkes PC, Ghirardello EJ, Allen R, Leitch VD, Butterfield NC, Komla-Ebri D, Adoum AT, Curry KF, White JK, Kussy F, Greenlaw KM, Xu C, Harvey NC, Cooper C, Adams DJ, Greenwood CMT, Maurano MT, Kaptoge S, Rivadeneira F, Tobias JH, Croucher PI, Ackert-Bicknell CL, Bassett JHD, Williams GR, Richards JB, Evans DM (2017) Identification of 153 new loci associated with heel bone mineral density and functional involvement of GPC6 in osteoporosis. Nat Genet 49: 1468–1475. https://doi.org/10.1038/ng.3949

Kim BJ, Ahn SH, Kim HM, Ikegawa S, Yang TL, Guo Y, Deng HW, Koh JM, Lee SH (2016) Replication of caucasian loci associated with osteoporosis-related traits in East Asians. J Bone Metab 23: 233–242. https://doi.org/10.11005/jbm.2016.23.4.233

Kurihara M, Shiraishi A, Satake H, Kimura AP (2014) A conserved noncoding sequence can function as a spermatocyte-specific enhancer and a bidirectional promoter for a ubiquitously expressed gene and a testis-specific long noncoding RNA. J Mol Biol 426: 3069–3093. https://doi.org/10.1016/j.jmb.2014.06.018

Liang WC, Fu WM, Wang YB, Sun YX, Xu LL, Wong CW, Chan KM, Li G, Waye MM, Zhang JF (2016) H19 activates Wnt signaling and promotes osteoblast differentiation by functioning as a competing endogenous RNA. Sci Rep 6:20121. https://doi.org/10.1038/srep20121

Liu X, Yang W, Li Y, Li S, Zhou X, Zhao Q, Fan Y, Lin M, Chen R (2016) The intergenic region of the maize defensin-like protein genes Def1 and Def2 functions as an embryo-specific asymmetric bidirectional promoter. J Exp Bot 67:4403–4413. https://doi.org/10.1093/jxb/erw226

Neer RM, Arnaud CD, Zanchetta JR, Prince R, Gaich GA, Reginster JY, Hodsman AB, Eriksen EF, Ish-Shalom S, Genant HK, Wang O, Mitlak BH (2001) Effect of parathyroid hormone (1–34) on fractures and bone mineral density in postmenopausal women with osteoporosis. N Engl J Med 344: 1434–1441. https://doi.org/10.1056/NEJM200105103441904

Park SE, Oh KW, Lee WY, Baek KH, Yoon KH, Son HY, Lee WC, Kang MI (2014) Association of osteoporosis susceptibility genes with bone mineral density and bone metabolism related markers in Koreans: the Chungju metabolic disease cohort (CMC) study. Endocr J 61:1069–1078. https://doi.org/10.1507/endocrj.EJ14-0119

Powell JE, Fung JN, Shakhbazov K, Sapkota Y, Cloonan N, Hemani G, Hillman KM, Kaufmann S, Luong HT, Bowdler L, Painter JN, Holdsworth-Carson SJ, Visscher PM, Dinger ME, Healey M, Nyholt DR, French JD, Edwards SL, Rogers PA, Montgomery GW (2016) Endometriosis risk alleles at 1p36.12 act through inverse regulation of CDC42 and LINC00339. Hum Mol Genet 25:5046–5058. https://doi.org/10.1093/hmg/ddw320

Qin L, Liu Y, Wang Y, Wu G, Chen J, Ye W, Huang Q (2016) Computational characterization of osteoporosis associated SNPs and genes identified by genome-wide association studies. PLoS One 11:e0150070. https://doi.org/10.1371/journal.pone.0150070

Ralston SH, Uitterlinden AG (2010) Genetics of osteoporosis. Endocr Rev 31:629–662. https://doi.org/10.1210/er.2009-0044

Richards JB, Rivadeneira F, Inouye M, Pastinen TM, Soranzo N, Wilson SG, Andrew T, Falchi M, Gwilliam R, Ahmadi KR, Valdes AM, Arp P, Whittaker P, Verlaan DJ, Jhamai M, Kumanduri V, Moorhouse M, van Meurs JB, Hofman A, Pols HA, Hart D, Zhai G, Kato BS, Mullin BH, Zhang F, Deloukas P, Uitterlinden AG, Spector TD (2008) Bone mineral density, osteoporosis, and osteoporotic fractures: a genome-wide association study. Lancet 371:1505–1512. https://doi.org/10.1016/S0140-6736(08)60599-1

Rivadeneira F, Styrkársdottir U, Estrada K, Halldórsson BV, Hsu YH, Richards JB, Zillikens MC, Kavvoura FK, Amin N, Aulchenko YS, Cupples LA, Deloukas P, Demissie S, Grundberg E, Hofman A, Kong A, Karasik D, van Meurs JB, Oostra B, Pastinen T, Pols HA, Sigurdsson G, Soranzo N, Thorleifsson G, Thorsteinsdottir U, Williams FM, Wilson SG, Zhou Y, Ralston SH, van Duijn CM, Spector T, Kiel DP, Stefansson K, Ioannidis JP, Uitterlinden AG, Genetic Factors for Osteoporosis (GEFOS) Consortium (2009) Twenty bone-mineral-density loci identified by large-scale meta-analysis of genome-wide association studies. Nat Genet 41:1199–1206. https://doi.org/10.1038/ng.446

Sato K, Suematsu A, Nakashima T, Takemoto-Kimura S, Aoki K, Morishita Y, Asahara H, Ohya K, Yamaguchi A, Takai T, Kodama T, Chatila TA, Bito H, Takayanagi H (2006) Regulation of osteoclast differentiation and function by the CaMK–CREB pathway. Nat Med 12: 1410–1416. https://doi.org/10.1038/nm1515

Streeten EA, McBride DJ, Pollin TI, Ryan K, Shapiro J, Ott S, Mitchell BD, Shuldiner AR, O'Connell JR (2006) Quantitative trait loci for bone mineral density identified by autosome-wide linkage scan to chromosomes 7q and 21q in men from the Amish Family Osteoporosis Study. J Bone Miner Res 21:1433–1442. https://doi.org/10.1359/jbmr.060602

Styrkarsdottir U, Halldorsson BV, Gretarsdottir S, Gudbjartsson DF, Walters GB, Ingvarsson T, Jonsdottir T, Saemundsdottir J, Center

JR, Nguyen TV, Bagger Y, Gulcher JR, Eisman JA, Christiansen C, Sigurdsson G, Kong A, Thorsteinsdottir U, Stefansson K (2008) Multiple genetic loci for bone mineral density and fractures. N Engl J Med 358:2355–2365. https://doi.org/10.1056/NEJMoa0801197

Styrkarsdottir U, Halldorsson BV, Gretarsdottir S, Gudbjartsson DF, Walters GB, Ingvarsson T, Jonsdottir T, Saemundsdottir J, Snorradóttir S, Center JR, Nguyen TV, Alexandersen P, Gulcher JR, Eisman JA, Christiansen C, Sigurdsson G, Kong A, Thorsteinsdottir U, Stefansson K (2009) New sequence variants associated with bone mineral density. Nat Genet 41:15–17. https://doi.org/10.1038/ng.284

Swarthout JT, Doggett TA, Lemker JL, Partridge NC (2001) Stimulation of extracellular signal-regulated kinases and proliferation in rat osteoblastic cells by parathyroid hormone is protein kinase C-dependent. J Biol Chem 276:7586–7592. https://doi.org/10.1074/jbc.M007400200

Wada T, Nakashima T, Hiroshi N, Penninger JM (2006) RANKL–RANK signaling in osteoclastogenesis and bone disease. Trends Mol Med 12:17–25. https://doi.org/10.1016/j.molmed.2005.11.007

Wang Y, He H, Li W, Phay J, Shen R, Yu L, de la Chapelle A (2017a) MYH9 binds to lncRNA gene PTCSC2 and regulates FOXE1 in the 9q22 thyroid cancer risk locus. Proc Natl Acad Sci USA 114: 474–479. https://doi.org/10.1073/pnas.1619917114

Wang Q, Li Y, Zhang Y, Ma L, Lin L, Meng J, Jiang L, Wang L, Zhou P, Zhang Y (2017b) LncRNA MEG3 inhibited osteogenic differentiation of bone marrow mesenchymal stem cells from postmenopausal osteoporosis by targeting miR-133a-3p. Biomed Pharmacother 89: 1178–1186. https://doi.org/10.1016/j.biopha.2017.02.090

Warrington NM, Kemp JP, Tilling K, Tobias JH, Evans DM (2015) Genetic variants in adult bone mineral density and fracture risk genes are associated with the rate of bone mineral density acquisition in adolescence. Hum Mol Genet 24:4158–4166. https://doi.org/10.1093/hmg/ddv143

Wuerfel C, Hoffmann C, Kawelke N, Aszodi A, Nakchbandi I (2012) Deletion of cdc42 in osteoblast progenitors leads to increased adipocyte differentiation and decreased bone formation. Bone 50:S43. https://doi.org/10.1016/j.bone.2012.02.113

Xu Y, Wang S, Tang C, Chen W (2015) Upregulation of long noncoding RNA HIF 1α-anti-sense 1 induced by transforming growth factor-β-mediated targeting of sirtuin 1 promotes osteoblastic differentiation of human bone marrow stromal cells. Mol Med Rep 12: 7233–7238. https://doi.org/10.3892/mmr.2015.4415

Yu B, Chang J, Liu Y, Li J, Kevork K, Al-Hezaimi K, Graves DT, Park NH, Wang CY (2014) Wnt4 signaling prevents skeletal aging and inflammation by inhibiting nuclear factor-[kappa] B. Nat Med 20:1009–1017. https://doi.org/10.1038/nm.3586

Zhang J, Glatfelter AA, Taetle R, Trent JM (1999) Frequent alterations of evolutionarily conserved regions of chromosome 1 in human malignant melanoma. Cancer Genet Cytogenet 111: 119–123. https://doi.org/10.1016/S0165-4608(98)00196-4

Zhang L, Choi HJ, Estrada K, Leo PJ, Li J, Pei YF, Zhang Y, Lin Y, Shen H, Liu YZ, Liu Y, Zhao Y, Zhang JG, Tian Q, Wang YP, Han Y, Ran S, Hai R, Zhu XZ, Wu S, Yan H, Liu X, Yang TL, Guo Y, Zhang F, Guo YF, Chen Y, Chen X, Tan L, Zhang L, Deng FY, Deng H, Rivadeneira F, Duncan EL, Lee JY, Han BG, Cho NH, Nicholson GC, McCloskey E, Eastell R, Prince RL, Eisman JA, Jones G, Reid IR, Sambrook PN, Dennison EM, Danoy P, Yerges-Armstrong LM, Streeten EA, Hu T, Xiang S, Papasian CJ, Brown MA, Shin CS, Uitterlinden AG, Deng HW (2014) Multistage genome-wide association meta-analyses identified two new loci for bone mineral density. Hum Mol Genet 23:1923–1933. https://doi.org/10.1093/hmg/ddt575

Zheng HF, Forgetta V, Hsu YH, Estrada K, Rosello-Diez A, Leo PJ, Dahia CL, Park-Min KH, Tobias JH, Kooperberg C, Kleinman A, Styrkarsdottir U, Liu CT, Uggla C, Evans DS, Nielson CM, Walter K, Pettersson-Kymmer U, McCarthy S, Eriksson J, Kwan T, Jhamai M, Trajanoska K, Memari Y, Min J, Huang J, Danecek P, Wilmot B, Li R, Chou WC, Mokry LE, Moayyeri A, Claussnitzer M, Cheng CH, Cheung W, Medina-Gómez C, Ge B, Chen SH,Choi K, Oei L, Fraser J, Kraaij R, Hibbs MA, Gregson CL, Paquette D, Hofman A, Wibom C, Tranah GJ, Marshall M, Gardiner BB, Cremin K, Auer P, Hsu L, Ring S, Tung JY, Thorleifsson G, Enneman AW, van Schoor NM, de Groot LC, van der Velde N, Melin B, Kemp JP, Christiansen C, Sayers A, Zhou Y, Calderari S, van Rooij J, Carlson C, Peters U, Berlivet S, Dostie J, Uitterlinden AG, Williams SR, Farber C, Grinberg D, LaCroix AZ, Haessler J, Chasman DI, Giulianini F, Rose LM, Ridker PM, Eisman JA, Nguyen TV, Center JR, Nogues X, Garcia-Giralt N, Launer LL, Gudnason V, Mellström D, Vandenput L, Amin N, van Duijn CM, Karlsson MK, Ljunggren Ö, Svensson O, Hallmans G, Rousseau F, Giroux S, Bussière J, Arp PP,Koromani F, Prince RL, Lewis JR, Langdahl BL, Hermann AP, Jensen JE, Kaptoge S, Khaw KT, Reeve J, Formosa MM, Xuereb-Anastasi A, Åkesson K, McGuigan FE, Garg G, Olmos JM, Zarrabeitia MT, Riancho JA, Ralston SH, Alonso N, Jiang X, Goltzman D, Pastinen T, Grundberg E, Gauguier D, Orwoll ES, Karasik D, Davey-Smith G, AOGC Consortium,Smith AV, Siggeirsdottir K, Harris TB, Zillikens MC, van Meurs JB, Thorsteinsdottir U, Maurano MT, Timpson NJ, Soranzo N, Durbin R, Wilson SG, Ntzani EE, Brown MA, Stefansson K, Hinds DA, Spector T, Cupples LA, Ohlsson C, Greenwood CM, UK10K Consortium, Jackson RD, Rowe DW, Loomis CA, Evans DM, Ackert-Bicknell CL, Joyner AL, Duncan EL, Kiel DP,Rivadeneira F, Richards JB (2015) Whole-genome sequencing identifies EN1 as a determinant of bone density and fracture. Nature 526:112–117. https://doi.org/10.1038/nature14878

Zheng J, Huang X, Tan W, Yu D, Du Z, Chang J, Wei L, Han Y, Wang C, Che X, Zhou Y, Miao X, Jiang G, Yu X, Yang X, Cao G, Zuo C, Li Z, Wang C, Cheung ST, Jiam Y, Zheng X, Shen H, Wu C, Lin D (2016) Pancreatic cancer risk variant in LINC00673 creates a miR-1231 binding site and interferes with PTPN11 degradation. Nat Genet 48:747–757. https://doi.org/10.1038/ng.3568